

Depth-selective ^{57}Fe conversion-electron Mössbauer spectroscopy. II. Experimental test—angular effects, accuracy

D. Liljequist and M. Ismail

Department of Physics, University of Stockholm, Vanadisvägen 9, S-113 46 Stockholm, Sweden

K. Saneyoshi,* K. Debusmann, W. Keune, R. A. Brand, and W. Kiauka

Laboratory of Applied Physics, University of Duisburg, Lotharstrasse 65, D-4100 Duisburg, Federal Republic of Germany

(Received 20 September 1984)

An experimental investigation of the depth and surface selectivity in depth-selective ^{57}Fe conversion-electron Mössbauer spectroscopy (DCEMS) has been performed by using a high-resolution electron-energy analyzer combined with a Mössbauer spectrometer. DCEMS spectra have been recorded in ultrahigh vacuum at different electron energies E from 6.5 to 7.3 keV (with 2.7% energy resolution) and, for the first time, at different electron-emission angles θ relative to the absorber surface normal (from $\theta=10^\circ$ to 72°), using a test absorber consisting of a thin α -Fe layer on a thick stainless-steel substrate. The α -Fe and stainless-steel Mössbauer spectral areas were found to be in very good agreement with theoretically calculated values. The predicted angular effects are verified; in particular, it is confirmed that the surface signal is enhanced by measuring at glancing angles relative to the absorber surface.

I. INTRODUCTION

Depth-selective ^{57}Fe conversion-electron Mössbauer spectroscopy (DCEMS) is a rapidly developing technique for the nondestructive investigation of ^{57}Fe -containing solid surface layers.¹ In DCEMS, electrons emerging from the surface of a Mössbauer absorber are detected by means of an electron spectrometer of several-percent resolution, and Mössbauer electron scattering spectra are obtained at different electron energies. Monoenergetic conversion electrons are emitted after the deexcitation of Mössbauer nuclei (e.g., 7.3-keV K conversion electrons in the case of ^{57}Fe), and their energy loss is related to their depth of origin below the surface of the Mössbauer absorber. In this way, information on the depth dependence of local physical parameters can be obtained. So far DCEMS has found applications in various fields of materials science, such as oxidation and corrosion,²⁻⁷ ion implantation,⁸⁻¹¹ surface and thin-film magnetism,¹²⁻¹⁶ and thin-film interdiffusion.¹⁷ It has been demonstrated that depth-selective surface studies in a region 0–1000 Å are feasible by using ^{57}Fe K conversion electrons.¹⁸ Furthermore, it can be concluded from experiments that detection of electrons emerging at glancing angles ($\approx 10^\circ$ – 20°) relative to the absorber surface leads to enhanced surface selectivity,^{14,16} an observation which appears important, for example, for the study of surface magnetism.

The present investigation is an extension of our previous work^{18,19} in order to compare the theoretical calculations presented in paper I of this series²⁰ with experimental results, and, in particular, a verification of the predicted angular effects. Therefore, a series of DCEMS measurements at different electron energies E and electron-emission angles θ (relative to the sample surface normal) have been performed on a ^{57}Fe Mössbauer test absorber consisting of an α - ^{57}Fe layer deposited on a stainless-steel

backing. CEMS and DCEMS test measurements on such absorbers have been carried out previously on several occasions for the same purposes as here, i.e., to check or obtain depth or [for conversion-electron Mössbauer spectroscopy (CEMS)] surface selectivity.^{18,21} This is, however, the first systematic investigation over angles as well as energies.

The notations used in paper I will be followed, with the modification that we will write $T_{\theta,V}^K(x)$ for the K -conversion-electron weight function obtained in the angular interval indicated by θ and at the electron spectrometer setting V . The setting value refers to the following to the nominal electron energy (in keV) as given by our spectrometer; in order to obtain a relation between the true electron energy E and V a calibration procedure will be described below. Theory [i.e., the data sets $T^K(x,G,E)$ and $T^L(x,G,E)$ simulated by the MC-II model as described in paper I] and experiment will be compared with respect to the (relative) values of the DCEMS signal $I_{\theta,V}$, which is defined as the Mössbauer (DCEMS) spectral area, obtained at the angle (angular interval) θ and the setting V , normalized to the total measuring time for the spectrum and corrected for nonresonant background and for decreasing source activity.

II. EXPERIMENTAL

A. Apparatus

The measurements were carried out with a modified commercial electrostatic (150° spherical sector) electron analyzer combined with conventional Mössbauer instrumentation.²² Figure 1 shows the chosen geometry of the experimental arrangement for the present measurement. It consists of a Rh ^{57}Co Mössbauer source (≈ 80 mCi initial activity) and a Mössbauer absorber (sample) which can be tilted (in UHV) so as to make different

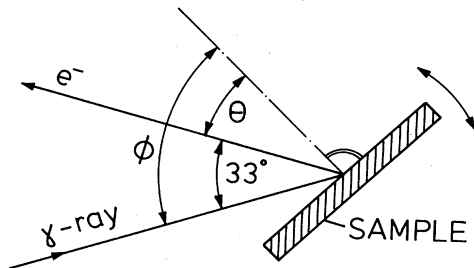


FIG. 1. Experimental geometry chosen for the present investigation. θ equals the angle between electron-emission direction and sample surface normal. ϕ equals the angle between 14.4 γ -ray direction and sample surface normal.

angles θ relative to the entrance aperture of the electron spectrometer (and simultaneously different angles relative to the γ -ray direction), all parts being placed in UHV (base pressure 5×10^{-11} Torr). The width $\Delta\theta$ of the angular interval selected by the analyzer is approximately $\pm 6^\circ$.

B. Spectrometer calibration

The spectrometer profile $S(V, E)$, i.e., the spectral shape on the spectrometer setting (V -) axis for monoenergetic electrons of energy E , was determined by measuring (*in situ*) the DCEMS signals $I_{\theta, V}$ from a Mössbauer absorber consisting of a 30 ± 5 Å α - ^{57}Fe layer vacuum deposited (in UHV) on an epitaxial 1200 Å thick (100) ^{56}Fe film on a LiF (100) substrate. DCEMS spectra were taken at several settings V near the nominal energy 7.3 keV at an angle $\theta = 15^\circ$ (almost perpendicular electron emission). These spectra (measured at room temperature) showed the typical magnetically split six-line pattern of α -Fe with slightly reduced hyperfine-field values as compared to bulk α -Fe.¹⁶ The DCEMS signal is, for this absorber, given by

$$I_{\theta, V} \propto \int_0^{30 \text{ \AA}} T_{\theta, V}^K(x) dx, \quad (1)$$

where $\theta = 15^\circ \pm 6^\circ$. The weight functions $T_{\theta, V}^K(x)$ are given by Eq. (1) in paper I. Comparing, by means of the program SPCONV mentioned in paper I, the experimental $I_{\theta, V}$ values with those calculated by Eq. (1), $S(V, E)$ is determined with respect to its shape (i.e., apart from a multiplicative factor). The resonant surface layer (30 Å ^{57}Fe) is thin enough to ensure that the calibration is not appreciably affected by electron-energy loss in the absorber, i.e., the observed I_V profile corresponds very closely to $S(V, E)$ itself.

Calibration data are shown in Fig. 2. It is seen that the positions of the measured points I_V are consistent with a triangular shape of the distribution $S(V, E)$ [Eq. (5) in paper I] with the full width at half maximum (FWHM) energy resolution 2.7%. The calibration constant V/E [(spectrometer setting)/(electron energy)] was found to be 1.007. (In this context it might be noted that the initial energy of the K conversion electrons is, in the Monte Car-

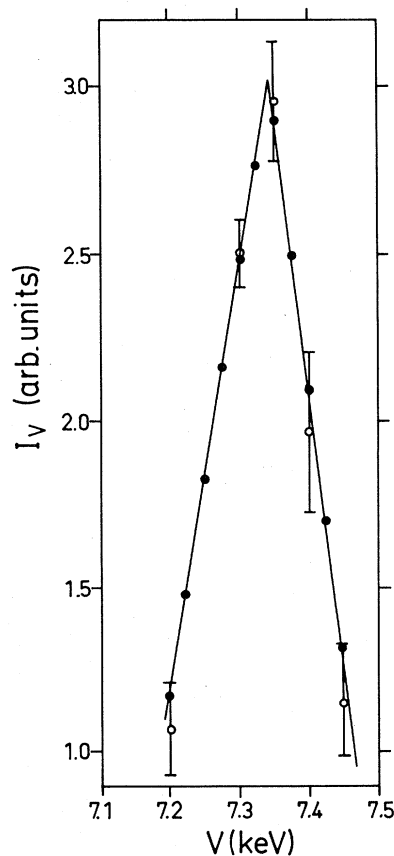


FIG. 2. Experimental (O) and theoretical (●) DCMS signal $I_{\theta, V}$ vs spectrometer setting V for $\theta = 15^\circ \pm 6^\circ$, obtained from a 30-Å-thick α - ^{57}Fe film.

to simulations described in paper I, assumed to be precisely 7.3 keV.) It should be noted that the V/E value is, in the practical analysis, the most important quantity to be obtained accurately by the calibration. In general, it is not necessary to use very thin electron sources for the calibration; it was made here in order to obtain a calibration which is, as far as possible, independent of the theoretically calculated electron scattering and energy loss.

With the spectrometer response function $S(V, E)$ thus obtained, K conversion-electron weight functions $T_{\theta, V}^K(x)$ for different angular intervals have been computed as described in paper I. It is found that the same $S(V, E)$ function applies at all angles; however, the multiplicative factor mentioned above changes with θ , due to a change in the (apparent) luminosity of the spectrometer as the absorber is rotated; actually, with our spectrometer,²² the luminosity increases markedly when the absorber is turned to a glancing-angle (large- θ) position.²³ This does not, however, affect the comparison of α -Fe and stainless-steel signals from the same absorber at a given angle. Examples of the K conversion-electron weight functions thus obtained for the present spectrometer, with the absorber oriented at different angles θ , are shown in Fig. 3.

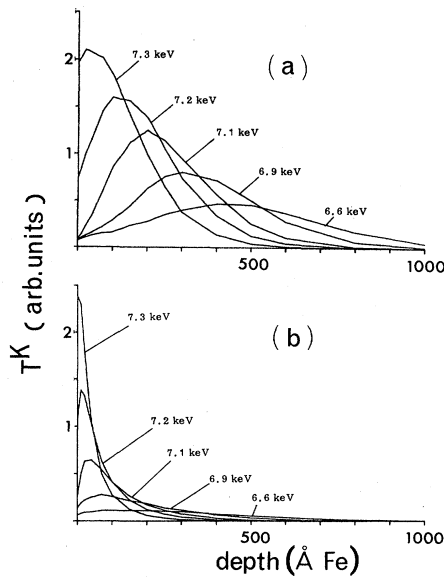


FIG. 3. Some typical theoretical K conversion-electron weight functions $T_{\theta, V}^K(x)$ calculated for the present spectrometer (2.7% FWHM energy resolution). Curves are labeled by setting (V) value, corresponding to energy E by $V/E=1.007$. The selected angular interval is $\theta=10^\circ \pm 6^\circ$ in (a) and $\theta=72^\circ \pm 6^\circ$ in (b). Depth (x) is measured in $\text{Å Fe}=0.0786 \mu\text{g}/\text{cm}^2$.

C. Test absorber

The (α -Fe)/(stainless-steel) Mössbauer absorber was prepared by UHV deposition of an α - ^{57}Fe layer (enriched to 95.3%, purity 99.9%) on a thick foil (2.5 μm) of 310 stainless steel (90.6% enriched in ^{57}Fe). The thickness of the α -Fe layer was measured by a quartz-crystal oscillator monitor, calibrated by an x-ray fluorescence measurement, to be $210 \pm 10 \text{ Å}$. Prior to film deposition the stainless-steel foil was surface cleaned by 5-kV argon-ion sputtering. During evaporation the maximum pressure was 1×10^{-8} Torr at an ^{57}Fe evaporation rate of 1 $\text{Å}/\text{s}$. The composition of the stainless-steel foil, as given by the manufacturer (NEN chemicals), was 57% Fe, 25% Cr, 14% Ni, 2% Mn, 1.5% Si, and residual C, P, and S.

An important quantity (see below) is the effective ^{57}Fe density n_{eff} in the absorber,²⁴ defined as the number of ^{57}Fe nuclei per unit mass thickness, multiplied by the recoil-free fraction (f factor). The stainless-steel (ss) chemical composition is such that, assuming equal recoil-free fractions, the effective ^{57}Fe densities $n_{\text{eff}}^{\text{Fe}}$ and $n_{\text{eff}}^{\text{ss}}$ in the α -Fe layer and the stainless steel, respectively, are related by $n_{\text{eff}}^{\text{Fe}}/n_{\text{eff}}^{\text{ss}}=1.85$.

D. Experimental results

The DCEMS spectra of the (α -Fe)/(stainless-steel) absorber were measured *in situ* at angles $\theta=10^\circ$, 46° , 60° , and 72° and, in each case, at spectrometer settings $V=7.3$, 7.2, 7.1, 6.9, 6.6, and 6.5 keV (nominal energy). Thus, the measurements involve a total of 24 Mössbauer spectra. The measuring time per spectrum ranged between 14 and

58 h, depending on the spectrum (average total count rate ≈ 1 count/s). A typical sequence of DCEMS spectra obtained at $\theta=10^\circ$ (almost perpendicular electron emission) for settings (energies) between 7.3 and 6.6 keV are shown in Fig. 4. Clear experimental evidence for depth selectivity is found from these spectra, in agreement with earlier observations.¹⁸ Thus, the typical six-line spectrum from the α -Fe layer is clearly enhanced relative to the stainless-steel peak of the substrate if electrons of high energy (7.3 keV) are selected, while decreasing the electron-energy setting reduces the α -Fe film signal and enhances the stainless-steel peak intensity. A similar sequence, but measured at $\theta=72^\circ$, is shown in Fig. 5. Figure 6 shows a sequence of DCEMS spectra obtained at $V=7.2$ keV for different angles θ ; it is clear from Figs. 5 and 6 that the α -Fe film signal is drastically enhanced relative to the stainless-steel peak intensity if measurements at glancing electron emission ($\theta=72^\circ$) are performed. One may also note the almost complete separation of surface from bulk in the opposite extreme cases, i.e., $V=6.6$ keV, $\theta=10^\circ$ (Fig. 4), and $V=7.3$ keV, $\theta=72^\circ$ (Fig. 5). Each DCEMS spectrum was least-squares fitted to Lorentzian line shapes. DCEMS signals (spectral areas) $I_{\theta, V}^{\text{Fe}}$ and $I_{\theta, V}^{\text{ss}}$ for α -Fe and stainless steel, respectively, at the different angles θ and settings V , were determined from the fit. The results are summarized in Table I and also plotted in Fig. 7 together with theoretical values calculated as described below. The typical FWHM was 0.45 mm/s for the α -Fe lines and 0.46 mm/s for the stainless-steel line. It should be mentioned that an integral CEMS measurement on our sample, obtained with the sample placed in a He- CH_4

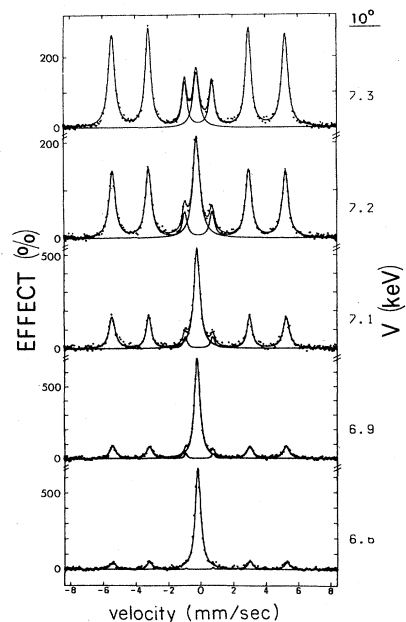


FIG. 4. DCEMS spectra at $\theta=10^\circ$ (almost perpendicular electron emission) for various electron-energy settings V between 7.3 and 6.6 keV, obtained from the test absorber, i.e., a 210 ± 10 - Å -thick layer of α - ^{57}Fe (95% enriched) on a stainless-steel substrate (91% enriched).

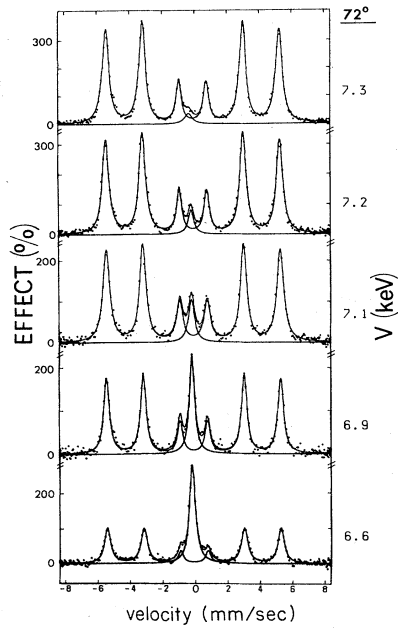


FIG. 5. DCEMS spectra at $\theta=72^\circ$ (near glancing-angle electron emission) for various electron-energy settings V , obtained from the same absorber as in Fig. 4.

flow-gas proportional counter, yielded a Mössbauer spectrum with relative spectral areas for α -Fe and stainless steel similar to those of our DCEMS measurement at $\theta=46^\circ$ and $V=6.5$ keV (Table I).

In Fig. 8 we have plotted experimental values of the "reduced" signal ratio $R_{\theta,V} = I_{\theta,V}^{\text{Fe}} / (I_{\theta,V}^{\text{Fe}} + 1.85 I_{\theta,V}^{\text{ss}})$. This quantity is useful, since it is fairly insensitive to the shape of the spectrometer profile.¹⁹ The factor 1.85 takes into account the different effective ^{57}Fe density in the

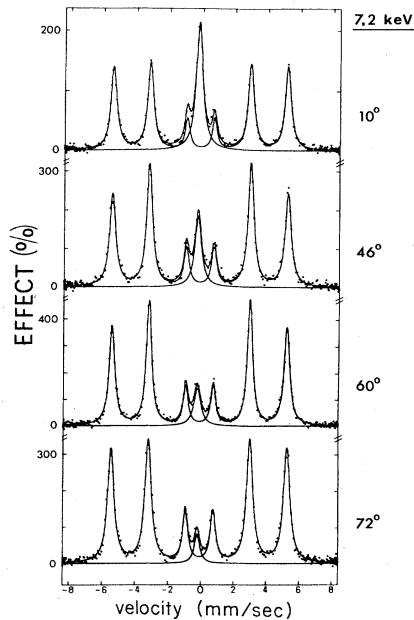


FIG. 6. DCEMS spectra at the electron-energy setting $V=7.2$ keV, for electron-emission angles $\theta=10^\circ, 46^\circ, 60^\circ,$ and 72° , obtained from the same absorber as in Figs. 4 and 5.

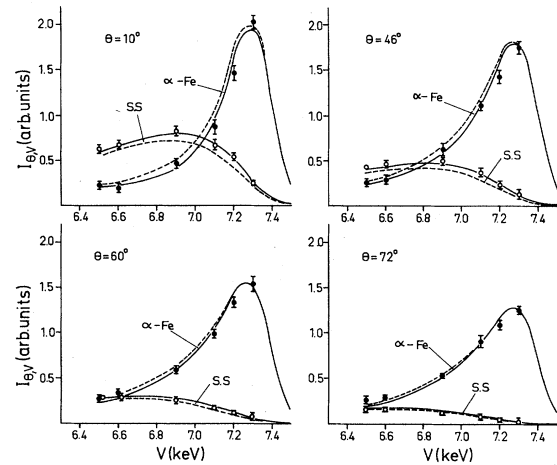


FIG. 7. Comparison between experimental and theoretical DCEMS signals for the same absorber as in Figs. 4–6. Experimental signals (Table I) from the α -Fe and stainless steel (ss) are shown by (\bullet) and (\circ) , respectively. Full curves show the DCEMS signals theoretically calculated by Eqs. 2(a)–2(c) from Monte Carlo simulated data on electron scattering and energy loss, assuming the α -Fe layer thickness $d=220$ Å. Dashed curves show the theoretically calculated result assuming $d=250$ Å.

TABLE I. Experimental DCEMS signals (in arbitrary units) $I_{\theta,V}^{\text{Fe}}$ and $I_{\theta,V}^{\text{ss}}$ for α -Fe and stainless steel, respectively (normalized to the corresponding measuring time and Mössbauer source activity, and corrected for nonresonant background), at different angles θ and electron-energy settings V (keV).

	V	I^{Fe}	I^{ss}
$\theta=10^\circ$	7.3	2.04 ± 0.07	0.25 ± 0.03
	7.2	1.48 ± 0.08	0.55 ± 0.04
	7.1	0.88 ± 0.08	0.68 ± 0.06
	6.9	0.47 ± 0.06	0.83 ± 0.05
	6.6	0.20 ± 0.04	0.68 ± 0.04
	6.5	0.24 ± 0.04	0.63 ± 0.05
$\theta=46^\circ$	7.3	1.76 ± 0.07	0.14 ± 0.05
	7.2	1.44 ± 0.08	0.24 ± 0.04
	7.1	1.12 ± 0.05	0.38 ± 0.04
	6.9	0.64 ± 0.07	0.51 ± 0.04
	6.6	0.30 ± 0.05	0.47 ± 0.04
	6.5	0.27 ± 0.04	0.44 ± 0.02
$\theta=60^\circ$	7.3	1.54 ± 0.08	0.08 ± 0.04
	7.2	1.34 ± 0.06	0.13 ± 0.02
	7.1	1.00 ± 0.05	0.17 ± 0.02
	6.9	0.61 ± 0.04	0.27 ± 0.03
	6.6	0.35 ± 0.04	0.30 ± 0.03
	6.5	0.28 ± 0.04	0.30 ± 0.02
$\theta=72^\circ$	7.3	1.26 ± 0.04	0.03 ± 0.05
	7.2	1.10 ± 0.05	0.05 ± 0.02
	7.1	0.91 ± 0.07	0.09 ± 0.03
	6.9	0.54 ± 0.03	0.13 ± 0.01
	6.6	0.30 ± 0.03	0.17 ± 0.01
	6.5	0.27 ± 0.04	0.17 ± 0.03

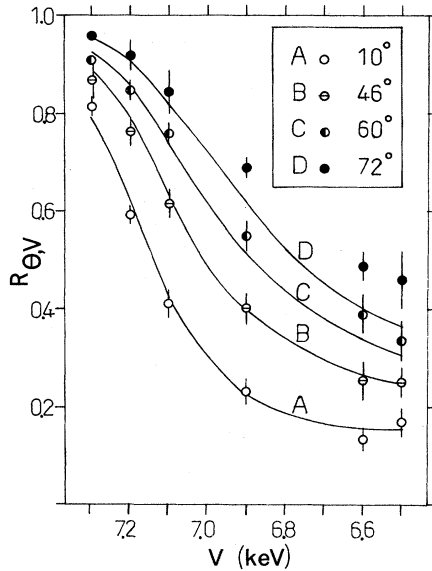


FIG. 8. Experimental and theoretical values of the reduced signal ratio $R_{\theta, \nu} = I_{\theta, \nu}^{\text{Fe}} / (I_{\theta, \nu}^{\text{Fe}} + 1.85 I_{\theta, \nu}^{\text{ss}})$ obtained for the (α -Fe)/(stainless-steel) absorber. The theoretical data (curves A–D) have been calculated assuming α -Fe layer thickness $d = 220$ Å. Values obtained from experimental data (Table I) are indicated by (\circ , \ominus , \bullet , \bullet).

α - ^{57}Fe film as compared to that in the stainless-steel foil; i.e., the signal ratio is reduced to the value obtained with a (fictitious) thick Mössbauer absorber, regarded as homogeneous with respect to the effective ^{57}Fe density.

III. ANALYSIS

A. Method

Theoretical DCEMS signals from the α -Fe and stainless-steel regions have, respectively, been calculated by

$$I_{\theta, \nu}^{\text{Fe}}(\text{theor}) = C \int_0^d n_{\text{eff}}^{\text{Fe}} T_{\theta, \nu}(x) \gamma_{\text{Fe}}(x) dx, \quad (2a)$$

$$I_{\theta, \nu}^{\text{ss}}(\text{theor}) = C \int_d^{\infty} n_{\text{eff}}^{\text{ss}} T_{\theta, \nu}(x) \gamma_{\text{ss}}(x) dx, \quad (2b)$$

where [with experimentally obtained signals denoted by “(expt)”]

$$C = \frac{\sum_{\nu} [I_{\theta, \nu}^{\text{Fe}}(\text{expt}) + I_{\theta, \nu}^{\text{ss}}(\text{expt})]}{\sum_{\nu} [I_{\theta, \nu}^{\text{Fe}}(\text{theor}) + I_{\theta, \nu}^{\text{ss}}(\text{theor})]} \quad (2c)$$

gives the scaling factor C , and where d is the thickness of the α -Fe layer. In the integration in Eqs. (2a) and (2b), depth (x) is, as mentioned in paper I, to be measured as (mass)/(area). $T_{\theta, \nu}$ is the appropriate sum of the K -conversion-electron (as exemplified in Fig. 3) and the L -conversion-electron weight functions in accordance with Eqs. (1)–(3) in paper I. In addition, there is a very small correction ($\approx 2\%$ increase) of the stainless-steel signal for the gamma conversion electron (GCE) contribution (secondary Mössbauer absorption—cf. Ref. 1); this has not been explicitly indicated in (2b). The factors $\gamma_{\text{Fe}}(x)$

and $\gamma_{\text{ss}}(x)$ take into account the resonant attenuation of the incident gamma radiation in the absorber. Non-resonant attenuation may be entirely neglected. The attenuation factors have been explicitly calculated by the formula

$$\gamma(x) = \sum_{j=1}^M \omega_j F(\omega_j x / \lambda \cos \phi), \quad (3)$$

where summation is made over the M Mössbauer lines in the spectrum, ω_j are the (normalized) statistical line weights, ϕ the incident radiation angle relative to the absorber surface normal, and λ the resonance attenuation length in Å Fe; a practical formula for the latter is

$$\lambda(\text{Å Fe}) = 620 / n_{\text{eff}}, \quad (4)$$

where n_{eff} is the effective ^{57}Fe density relative to that of 100% enriched α -Fe. The function F is defined by

$$F(z) = (2/\pi) \int_0^{\pi/2} \exp(-z \cos^2 y) dy, \quad (5)$$

which essentially is an integration over the Lorentzian line shape, cast into a form which permits rapid numerical integration.

In the present measurements the angle ϕ varied between 13° and 39° . To give an example, the calculated attenuation factor for the α -Fe phase decreases from 1, at the surface, to about 0.97 at the depth 250 Å, if the radiation is incident perpendicularly on the absorber surface. For the stainless-steel phase, the corresponding values are 1 at the interface (i.e., at depth 250 Å from the surface) and about 0.75 at a depth of 1000 Å from the surface.

It should be noted, however, that the L -conversion-electron and the GCE contributions, as well as the actual effect of the gamma-attenuation factors on the DCEMS signals $I_{\theta, \nu}$, are *small* corrections. (The gamma attenuation is appreciable only at depths from which the K -conversion-electron transmission is always small.) A good approximation (accurate to within a few percent) is in general—and here—obtained by including only the K -conversion-electron contribution and neglecting gamma attenuation entirely;²⁴ i.e., setting $T = T^K$ and $\gamma_{\text{Fe}} = \gamma_{\text{ss}} = 1$.

Assuming equal recoil-free fraction one has, as mentioned, $n_{\text{eff}}^{\text{Fe}} / n_{\text{eff}}^{\text{ss}} = 1.85$. The correctness of this may, neglecting gamma attenuation, be checked by using the “sum rule” of DCEMS,²⁴ which in the present case says that the value of

$$\left[\frac{I_{\theta, \nu}^{\text{Fe}}(\text{expt})}{n_{\text{eff}}^{\text{Fe}}} + \frac{I_{\theta, \nu}^{\text{ss}}(\text{expt})}{n_{\text{eff}}^{\text{ss}}} \right] \left[\int_0^{\infty} T_{\theta, \nu}(x) dx \right]^{-1} \quad (6)$$

should be independent of setting V (at a given angle). Taking $n_{\text{eff}}^{\text{ss}} = 1$, one may search the value of $n_{\text{eff}}^{\text{Fe}}$ which gives the minimum deviation from this rule. By this method, we have found that $n_{\text{eff}}^{\text{Fe}}$ should have the value 1.8 with an estimated uncertainty ± 0.1 . This confirms that the value 1.85 is in agreement with the experimental data; $n_{\text{eff}}^{\text{Fe}} = 1.85$ and $n_{\text{eff}}^{\text{ss}} = 1$ have been used in the analysis.

B. Results

It should be pointed out that the DCEMS signals, as functions of setting V , correspond (closely) to the energy-

loss distributions of K conversion electrons starting from random depths in the α -Fe and the stainless-steel regions, respectively, as measured by the present electron spectrometer. The agreement between experimental and theoretical $I_{\theta, \nu}^{\text{Fe}}$ and $I_{\theta, \nu}^{\text{ss}}$ values shown in Fig. 7 appears to be very good, and the predicted dependence on angle θ is very well confirmed by the experiment.

The best all-over least-squares fit of theoretically computed to experimental values is obtained with $d=220 \text{ \AA}$ in Eqs. (2a)–(2c), as shown in Fig. 7; this value agrees with the x-ray fluorescence measurement of the α -Fe layer thickness to within 5%. The sensitivity of the theoretically computed DCEMS signals to the value of d is apparent from the result for $d=250 \text{ \AA}$, which has also been plotted in Fig. 7. Actually, the fit at $\theta=72^\circ$ is slightly better for $d=250 \text{ \AA}$ (Fig. 7), but one should note that the thickness of the iron layer is more accurately determined at low θ (perpendicular measurement), since the (α -Fe)/(stainless-steel) interface lies rather deep below the surface, where depth resolution is better for low- θ values;²⁰ see Fig. 3.

The theoretical reduced signal ratio (Fig. 8) is in good agreement with the experimentally obtained values at $\theta=10^\circ$ and 46° . At $\theta=72^\circ$, and, to smaller extent, at $\theta=60^\circ$, the experimental value is somewhat larger at low energies ($<7 \text{ keV}$), i.e., the angular effect appears to be somewhat stronger here than predicted theoretically. Looking at Fig. 7, one may see that these deviations in Fig. 8 are due to very small differences in the DCEMS signals themselves. The theory may be tested more precisely in this region [large θ , low ($<7 \text{ keV}$) energies] by

repeating the present measurement with a thinner ($\approx 50 \text{ \AA}$) α -Fe layer. A possible reason for the observed deviation—though difficult to verify experimentally—might be surface roughness, which may be investigated theoretically by methods described elsewhere.²⁵

IV. SUMMARY

The depth and surface selectivity of ^{57}Fe DCEMS has been investigated using a Mössbauer test absorber consisting of a $210 \pm 10 \text{ \AA}$ α - ^{57}Fe layer deposited on a thick stainless-steel substrate. The measured energy and angular dependence of the DCEMS signals (Mössbauer spectral areas) was found to be in very good agreement with theoretical data obtained by Monte Carlo simulation of the electron scattering and energy loss. The surface (α - ^{57}Fe) signal was found to be strongly enhanced by measuring electrons at glancing angles relative to the absorber surface. The present experimental results suggest that the Monte Carlo computed weight functions are very reliable for the quantitative analysis of experimental DCEMS data.

ACKNOWLEDGMENTS

The authors appreciate helpful discussions with Dr. H. D. Pfannes. We are grateful to Dr. G. Bayreuther for the x-ray fluorescence measurement. Technical assistance by U. V. Hoersten and W. Weyers is gratefully acknowledged. This work was supported by the Deutsche Forschungsgemeinschaft.

*Present address: Department of Energy Sciences, Tokyo Institute of Technology, Nagatsuta, Midori-ku, Yokohama, Japan.

¹For a recent review, see D. Liljequist, in *Scanning Electron Microscopy III* (SEM Inc., AMF O'Hare, Chicago, 1983), pp. 997–1017.

²G. Belozerskii, C. Bohm, T. Ekdahl, and D. Liljequist, *Corros. Sci.* **22**, 831 (1982).

³C. Bohm, U. Bäverstam, B. Bodlund-Ringström, and D. Liljequist, University of Stockholm Report No. 79-07.

⁴G. N. Belozerskii, C. Bohm, T. Ekdahl, and D. Liljequist, *Nucl. Instrum. Methods* **192**, 539 (1982).

⁵M. Domke, B. Kyvelos, and G. Kaindl, *Surf. Sci.* **126**, 727 (1983).

⁶M. Domke and B. Kyvelos, *Corros. Sci.* **23**, 921 (1983).

⁷B. Bodlund-Ringström, U. Bäverstam, and C. Bohm, *J. Vac. Sci. Technol.* **16**, 1013 (1979).

⁸T. Shigematsu, S. Staniek, R. A. Brand, W. Keune, R. H. Nussbaum, H. D. Pfannes, D. Liljequist, G. Longworth, and R. Atkinson, *Hyperfine Interactions* **15/16**, 383 (1983).

⁹J. Itoh, Y. Yonekura, T. Toriyama, H. Miyasaka, and K. Hisatake, *Hyperfine Interactions* **15/16** 771 (1983).

¹⁰M. Carbuicchio, L. Bardani, and S. Tosto, *J. Appl. Phys.* **52**, 4589 (1981).

¹¹K. Saneyoshi, K. Debusmann, W. Keune, and D. Liljequist (unpublished), paper III in this series.

¹²K. Saneyoshi, T. Toriyama, J. Itoh, K. Hisatake, and S. Chikazumi, *J. Magn. Magn. Mater.* **31–34** 705 (1983).

¹³J. Itoh, Y. Yonekura, K. Saneyoshi, T. Toriyama, and K. Hisatake, *J. Magn. Magn. Mater.* **35**, 340 (1983).

¹⁴T. Yang, A. Krishnan, N. Benczer-Koller, and G. Bayreuther, *Phys. Rev. Lett.* **48**, 1292 (1982).

¹⁵S. Staniek, T. Shigematsu, W. Keune, and H.-D. Pfannes, *J. Magn. Magn. Mater.* **35**, 347 (1983).

¹⁶W. Kiauka, K. Debusmann, R. A. Brand, W. Keune, and N. Hosoito (unpublished).

¹⁷T. Shigematsu, S. Staniek, W. Keune, H.-D. Pfannes, and D. Liljequist, in *Proceedings of the International Conference on the Mössbauer Effect, Alma Ata, USSR, 1983* (Gordon and Breach, in press).

¹⁸T. Shigematsu, H.-D. Pfannes, and W. Keune, *Phys. Rev. Lett.* **45**, 1206 (1980).

¹⁹D. Liljequist, *Nucl. Instrum. Methods* **185**, 599 (1981).

²⁰D. Liljequist, and M. Ismail, preceding paper [*Phys. Rev. B* **31**, 4131 (1985)].

²¹M. J. Tricker, in *Mössbauer Spectroscopy and Its Chemical Applications, Advances in Chemistry Series, 194*, edited by J. G. Stevens and G. K. Shenoy (American Chemical Society, Washington, D.C., 1981), p. 63.

²²T. Shigematsu, H.-D. Pfannes, and W. Keune, in *Mössbauer Spectroscopy and Its Chemical Applications, Advances in Chemistry Series 194*, edited by J. G. Stevens and G. K. Shenoy (American Chemical Society, Washington, D.C., 1981), p. 125.

²³A. E. Hughes and C. C. Phillips, *Surf. Interface Anal.* **4**, 220 (1982).

²⁴D. Liljequist and B. Bodlund-Ringström, *Nucl. Instrum. Methods* **160**, 131 (1979).

²⁵D. Liljequist and M. Ismail (unpublished).